# Intratumoral STING Activation with T-cell Checkpoint Modulation Generates Systemic Antitumor Immunity

Casey R. Ager[1,2], Matthew J. Reilley[3], Courtney Nicholas[2], Todd Bartkowiak[1,2], Ashvin R. Jaiswal[1,2], and Michael A. Curran[1,2]

## Abstract

Coordinated manipulation of independent immune regulatory pathways in the tumor microenvironment—including blockade of T-cell checkpoint receptors and reversal of suppressive myeloid programs—can render aggressive cancers susceptible to immune rejection. Elevated toxicity associated with combination immunotherapy, however, prevents translation of the most efficacious regimens. We evaluated T-cell checkpoint–modulating antibodies targeting CTLA-4, PD-1, and 4-1BB together with myeloid agonists targeting either STING or Flt3 in the TRAMP-C2 model of prostate cancer to determine whether low-dose intratumoral delivery of these agents could elicit systemic control of multifocal disease. Intratumoral administration of the STING agonist cyclic di-GMP (CDG) or Flt3 Ligand (Flt3L) augmented the therapeutic effect of systemic triple checkpoint modulation and promoted the cure of 75% of mice with bilateral TRAMP-C2; however, when all agents were administered locally, only CDG mobilized abscopal immunity. Combination efficacy correlated with globally enhanced ratios of CD8$^+$ T cells to regulatory T cells (Treg), macrophages, and myeloid-derived suppressor cells, and downregulation of the M2 marker CD206 on tumor-associated macrophages. Flt3L improved CD8$^+$ T-cell and dendritic cell infiltration of tumors, but was diminished in efficacy by concomitant Treg expansion. Although intratumoral CDG/checkpoint therapy invokes substantial ulceration at the injection site, reduced CDG dosing can preserve tissue integrity without sacrificing therapeutic benefit. For high-order combinations of T-cell checkpoint antibodies and local myeloid agonists, systemic antibody administration provides the greatest efficacy; however, local administration of CDG and antibody provides substantial systemic benefit while minimizing the potential for immune-related adverse events. *Cancer Immunol Res; 5(8); 676–84. ©2017 AACR.*

## Introduction

Therapeutic blockade of T-cell coinhibitory receptors CTL-associated antigen 4 (CTLA-4) and programmed death 1 (PD-1) is sufficient to promote durable immune-mediated tumor regression across multiple cancers in mouse and man. Neither ipilimumab (anti–CTLA-4) nor nivolumab (anti–PD-1), however, provide clinical benefit in the setting of castration-resistant prostate cancer (CRPC; refs. 1, 2). Prostate cancer is the second leading cause of cancer-related death in men, and patients with CRPC have a median overall survival of 14 months, highlighting the urgent need for alternative immunotherapeutic approaches for this disease (3). Preclinical models of prostate cancer, including the transgenic adenocarcinoma of the mouse prostate (TRAMP) mouse and its derivative TRAMP-C2 implantable cell line (4),

reveal two major barriers to antitumor immunity in CRPC: (i) poor CD8$^+$ T-cell infiltration into the prostate tumor microenvironment (TME) and (ii) robust infiltration of immunosuppressive myeloid populations including tumor-associated macrophages (TAM) and myeloid-derived suppressor cells (MDSC). Given the well-described means by which TAM and MDSC impede T-cell infiltration and effector function independent of the CTLA-4/PD-1 axes (5), therapies which deplete or biologically reprogram TAM and MDSC may render the prostate TME amenable to T-cell activity. Absent these barriers to T-cell infiltration and function, we hypothesize that CRPC patients would be likely to experience durable benefit from T-cell checkpoint blockade.

In this study, we pursued a rational approach to design and evaluate multimodal therapies for CRPC consisting of antagonistic antibodies targeting T-cell coinhibitory receptors CTLA-4 and PD-1, agonistic antibodies targeting the T-cell costimulatory receptor 4-1BB, and agonistic molecules targeting myeloid activation pathways including stimulator of interferon induced genes (STING) or FMS-like tyrosine kinase 3 (Flt3). Our lab previously established synergistic relationships between anti–CTLA-4 and anti–PD-1 antibodies, owing to their nonredundant roles in regulating central T-cell priming and peripheral effector function (6). These data preceded successful phase III trials and subsequent FDA approval of this combination in patients with metastatic melanoma (7, 8). In addition, we described complimentary effects of CTLA-4 blockade with concomitant ligation of the stimulatory receptor 4-1BB, which promotes CD8$^+$ T-cell survival, proliferation, and TH1 cytokine production (9). In each setting,

[1]Immunology Program, University of Texas Graduate School of Biomedical Sciences at Houston, Houston, Texas. [2]Department of Immunology, University of Texas MD Anderson Cancer Center, Houston, Texas. [3]Division of Cancer Medicine, University of Texas MD Anderson Cancer Center, Houston, Texas.

**Note:** Supplementary data for this article are available at Cancer Immunology Research Online (http://cancerimmunolres.aacrjournals.org/).

**Corresponding Author:** Michael A. Curran, The University of Texas MD Anderson Cancer Center, 1515 Holcombe Blvd, Unit 0901, Houston, TX 77030. Phone: 713-563-3286; Fax: 713-563-3276; E-mail: mcurran@mdanderson.org

combination therapies were maximally effective in the context of an irradiated cellular vaccine secreting Flt3-ligand (Flt3L). Known for its classical role in promoting survival, proliferation, and differentiation of hematopoietic progenitors, Flt3L can induce dendritic cell (DC) chemotaxis and conversion to a $CD8\alpha^+CD103^+$ phenotype associated with cross-presentation and robust T-cell priming potential (10, 11). In contrast, Flt3L also promotes differentiation of plasmacytoid DCs, which can exert tolerogenic effects in cancer through induction of regulatory T cells (Treg) and limit the efficacy of Flt3L as a cancer immunotherapy (12).

The cytosolic nucleic acid sensor STING acts to promote tumor-specific T-cell responses by activating interferon secretion and costimulatory ligand expression by myeloid cells after uptake of tumor cell–derived DNA and is indispensable for spontaneous rejection of immunogenic cancers (13). Cyclic dinucleotide agonists of STING activate macrophages and DC in vitro and have demonstrated therapeutic utility alone and in combination with checkpoint blockade across multiple tumor models (14, 15).

Using mice bearing bilaterally implanted TRAMP-C2 tumors, we found that intratumoral STING activation with the dinucleotide cyclic di-GMP (CDG) mediates regression of injected tumors, but fails to elicit systemic "abscopal" immunity targeting distal lesions. Triple checkpoint modulation with anti–CTLA-4, anti–PD-1, and anti–4-1BB, however, converts intratumoral CDG into a potentiator of systemic immunity capable of rejecting distal, uninjected lesions. In contrast, intratumoral Flt3L augments the benefit of triple checkpoint modulation, but only when administered locally at each lesion. Given the potential toxicity of anti–CTLA-4, anti–PD-1, and anti–4-1BB combination therapy, we investigated whether intratumoral administration of this combination at low doses could serve as a safer alternative to systemic antibody therapy. These studies demonstrate that curative abscopal immunity can be generated against multifocal TRAMP-C2 when local triple checkpoint modulation is used in combination with intratumoral CDG. This therapeutic synergy is associated with infiltration of tumor-specific T cells and enhanced ratios of $CD8^+$ T cells to Treg, MDSC, and TAM, as well as pronounced downregulation of the M2 macrophage marker CD206 on TAM. Alternatively, Flt3L failed to mobilize abscopal immunity in combination with triple checkpoint modulation, likely due its expansion of $CD4^+$ Teff and Treg populations with similar potency to $CD8^+$ T cells at local and distal lesions. We observed dose-dependent skin pathology in mice receiving intratumoral CDG in combination with triple checkpoint blockade, although the therapeutic benefit of this combination appears modestly (but not significantly) dose-dependent. These data support the development of combinatorial strategies targeting adaptive and innate immune populations in prostate cancer, and inform the design of dosing strategies for STING agonists and checkpoint modulators to maximize clinical benefit while minimizing undue toxicity.

## Materials and Methods

### Mice

Male C57BL/6 mice were obtained from The Jackson Laboratory and were housed according to the Association for Assessment and Accreditation of Laboratory Animal Care and NIH standards. All experiments were conducted according to protocols approved by the University of Texas MD Anderson Cancer Center Institu-

tional Animal Care and Use Committee. Mice were approximately 8 weeks old at the time of tumor implantation.

### Antibodies

The following therapeutic antibodies were obtained from Bio X Cell and used in vivo at the indicated concentrations: anti–CTLA-4 (9H10; 100 μg i.p. 50 μg i.t.), anti–PD-1 (RMP1-14; 250 μg i.p. 50 μg i.t.), anti–4-1BB (3H3; 150 μg i.p. 50 μg i.t.). Antibodies used for flow cytometry were obtained from Biolegend, BD Biosciences, eBioscience, and Fisher Scientific and are described in Supplementary Table S1.

### Myeloid agonists

STING agonist c-di-GMP (CDG; Invivogen) was administered i.t. at 25 μg per mouse. Flt3L-Ig (Flt3L; Bio X Cell) was administered i.t. at 50 μg per mouse or 200 μg per mouse where described.

### Cell lines

The TRAMP-C2 tumor cell line was provided by Dr. Norman Greenberg, and all experiments in this article were performed using passage 21-22 tumor cells. TRAMP-C2 cells were maintained as previously described (4).

### TRAMP-C2 implantation and treatment

All mice were implanted at day 0 on both flanks with $1 \times 10^6$ TRAMP-C2 cells. For survival analysis experiments, mice were treated on days 14, 18, and 22 i.p. (100 μL volume) and/or i.t. (50–100 μL volume) with the indicated antibodies and myeloid agonists. Tumor volumes were measured with calipers to define the largest length ($a$), width ($b$), and height ($c$), and volumes were calculated as ($a$ x $b$ x $c$).

### Flow cytometry analysis of tumor immune infiltrate

TRAMP-C2 cells ($1 \times 10^6$) were mixed with 30% collagen matrix (Matrigel, BD) and implanted at day 0 on both flanks. Mice received treatment when tumors reached approximately 200 $mm^3$ volume, on days 31, 35, and 39. On day 42, mice were sacrificed, tumors excised, and digested with collagenase H (Sigma) and DNAse (Roche), then live infiltrating immune cells were purified by ficoll gradient centrifugation (Sigma; 1119 density). Cells were then fixed and permeabilized (eBioscience FoxP3 Fix/Perm kit), stained with fluorescently labeled antibodies, and analyzed by 18-color flow cytometry on a BD LSRII flow cytometer.

## Results

### Intratumoral CDG potentiates systemic checkpoint modulation in TRAMP-C2

In both clinical and preclinical settings, prostate cancer remains refractory to checkpoint blockade therapy targeting CTLA-4 or PD-1. To identify combinatorial strategies capable of sensitizing prostate tumors to immunotherapy, we augmented our checkpoint blockade cocktail of antagonistic anti–CTLA-4 and anti–PD-1 antibodies with an agonistic antibody targeting 4-1BB, a costimulatory receptor of the Tumor Necrosis Factor Receptor (TNFR) superfamily which promotes $CD8^+$ T-cell survival and cytotoxic effector function (16). We next investigated whether intratumoral STING activation using the STING agonist c-di-GMP (CDG) can potentiate checkpoint modulation by promoting
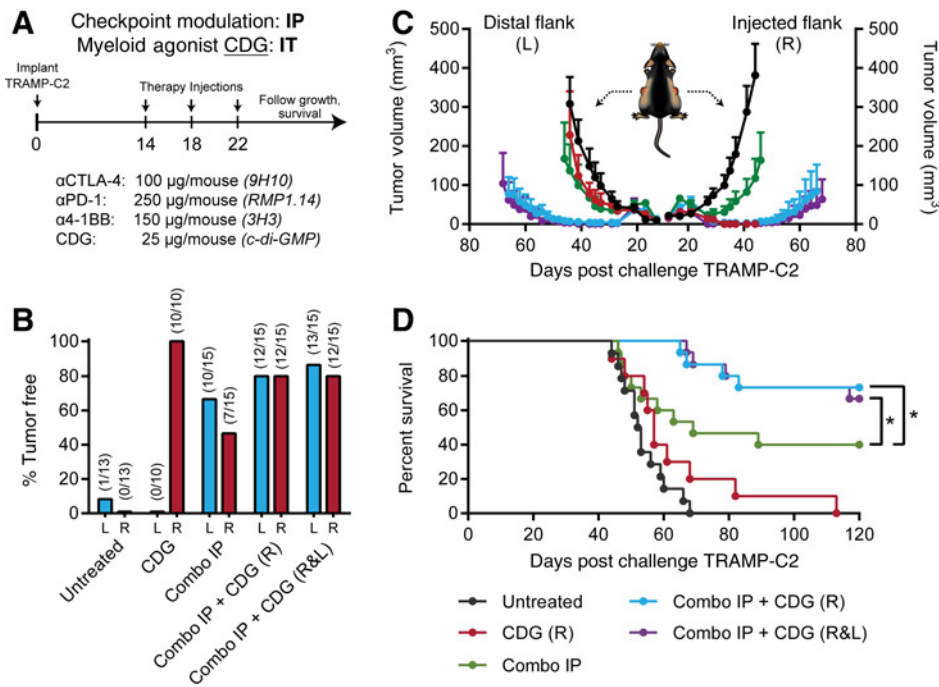
**Figure 1.**
Local CDG potentiates i.p. checkpoint modulation against bilateral TRAMP-C2. **A,** Five to 8-week-old C57BL/6 mice were challenged with $1 \times 10^6$ TRAMP-C2 cells on both flanks and were treated on days 14, 18, and 22 after implantation with i.p. checkpoint modulators and/or intratumoral (IT) CDG at either the right (R) or both right and left flank tumors (R and L). **B,** Percentage of mice tumor free at each flank, (**C**) tumor growth kinetics, and (**D**) overall survival over the treatment period are shown. Mice were deemed moribund when tumor volume reached 1,000 mm$^3$. Data are cumulative of $n = 3$ experiments with 5 mice per group. Statistical significance for survival was calculated using the Gehan–Breslow–Wilcoxon test. Ns, not significant; *, $P < 0.05$; **, $P < 0.01$; ***, $P < 0.001$; ****, $P < 0.0001$.

*in situ* vaccine-like augmentation of T-cell priming and proinflammatory reprogramming of the murine prostate tumor myeloid compartment. Mice were challenged with $1 \times 10^6$ TRAMP-C2 cells on both flanks, and received three doses of therapy every 4 days beginning when tumors were palpable on day 14. Tumor growth and survival were monitored until tumors reached 1,000 mm$^3$ (Fig. 1A). We found that as a single agent, intratumoral CDG mediated rejection of essentially all locally injected tumors; however, CDG failed to elicit a systemic immune response capable of clearing distal, uninjected lesions (Fig. 1B–C; Supplementary Fig. S2). Although systemic triple checkpoint modulation with anti–CTLA-4, anti–PD-1, and anti–4-1BB demonstrated efficacy in this model, curing both bilateral tumors in 40% of mice, we found that concurrent administration of CDG and immunotherapeutic antibodies, even at a single lesion, induced complete bilateral tumor rejection in approximately 75% of mice (Fig. 1D). This revealed a therapeutic synergy between CDG and our antibody cocktail and demonstrated the abscopal potential of
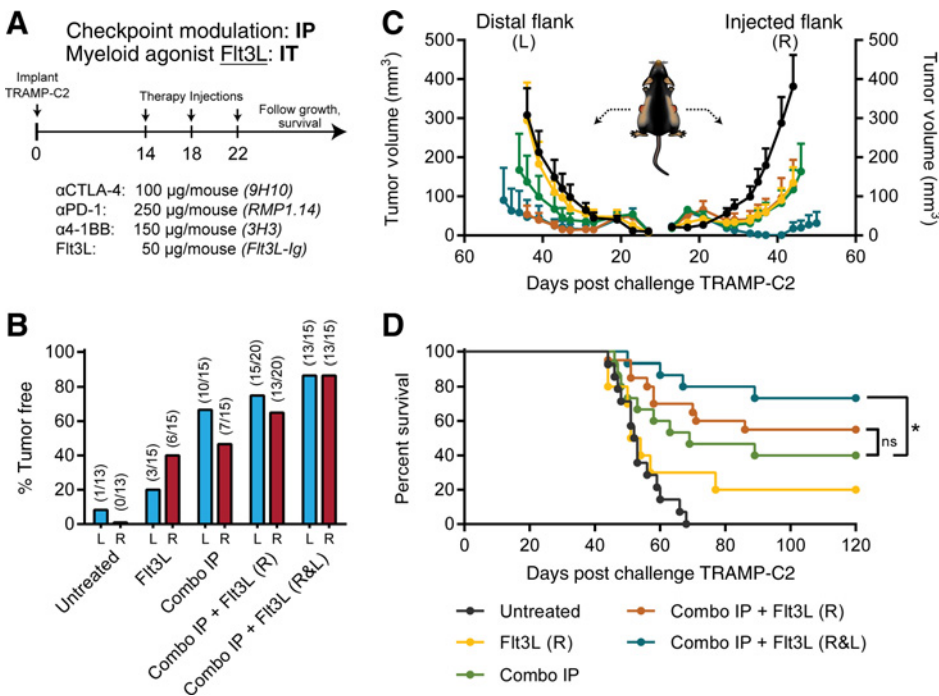


**Figure 2.**
Local Flt3L potentiates i.p. checkpoint modulation against bilateral TRAMP-C2. **A,** Five to eight-week-old C57BL/6 mice were challenged with $1 \times 10^6$ TRAMP-C2 cells on both flanks and were treated on days 14, 18, and 22 after implantation with i.p. checkpoint modulators and/or intratumoral (IT) Flt3L at either the right (R) or both right and left flank tumors (R and L). **B,** Percentage of mice tumor free at each flank, (**C**) tumor growth kinetics, and (**D**) overall survival over the treatment period are shown. Mice were deemed moribund when tumor volume reached 1,000 mm$^3$. Data are cumulative of $n = 3$ experiments with 5 mice per group. Statistical significance for survival was calculated using the Gehan–Breslow–Wilcoxon test. ns, not significant; *, $P < 0.05$; **, $P < 0.01$; ***, $P < 0.001$; ****, $P < 0.0001$.

CDG when combined with systemic checkpoint-modulating therapies.

## Intratumoral Flt3L at each lesion potentiates systemic checkpoint modulation in TRAMP-C2

Given our previous work combining checkpoint blockade with irradiated cellular vaccines secreting Flt3L (17), and the potential for Flt3L to act as a chemotactic and differentiation factor for DCs, we also chose to evaluate the capacity of intratumoral Flt3L to potentiate triple checkpoint modulation in our bilateral TRAMP-C2 model (Fig. 2A). In contrast to CDG, intratumoral Flt3L exhibited modest local efficacy as a single agent, yet achieved curative responses in approximately 15% of mice (Fig. 2B–D). Similar to CDG, Flt3L synergized with triple checkpoint modulation to cure 75% of mice in this model; however, this maximal response required intratumoral administration of Flt3L at each tumor (Fig. 2D). Therefore, in optimal conditions, Flt3L and CDG were capable of potentiating triple checkpoint modulation with similar efficacy, curing up to 75% of mice with multifocal, poorly immunogenic TRAMP-C2 tumors. When combined with systemic checkpoint modulators, however, only the STING agonist mobilized abscopal immunity.

## Intratumoral checkpoint modulation and CDG mobilizes abscopal immunity

In the clinic, individual checkpoint modulators can trigger severe, dose-limiting immune-related adverse events in many patients (18). Colitis, pruritus, fatigue, and rash are toxicities associated with anti–CTLA-4 and anti–PD-1. Agonistic antibodies targeting 4-1BB are associated with rare instances of fatal hepatotoxicity (19–21). Therefore, combinatorial strategies to target CTLA-4, PD-1, and 4-1BB must be suboptimally dosed or administered in a manner that limits systemic toxicity while preserving therapeutic potency. Based on a number of studies investigating intratumoral administration of checkpoint modulators including anti–CTLA-4 (22, 23), we asked whether intratumoral adminis-

tration of low-dose combination checkpoint modulation with anti–CTLA-4, anti–PD-1, and anti–4-1BB could prime local and systemic immunity against bilateral TRAMP-C2, and whether concomitant local STING activation with CDG could further potentiate these effects.

Mice bearing 14-day established bilateral TRAMP-C2 tumors received three intratumoral injections of therapy only at the right flank tumor 4 days apart (Fig. 3A). In this setting, intratumoral low-dose anti–CTLA-4, anti–PD-1, and anti–4-1BB mediated regression of approximately 50% of injected tumors, but failed to engender systemic immunity against distal lesions (Fig. 3B–D; Supplementary Fig. S3). Concurrent administration of CDG augmented the abscopal potential of local checkpoint modulation, however, promoting abscopal regression of distal lesions and bilateral tumor rejection in up to 52% of mice. In this setting, we did not observe a statistically significant dose-dependent increase in efficacy with additional CDG doses in potentiating local checkpoint modulation (Fig. 3D). Thus, we conclude that one or more doses of CDG can enhance the curative abscopal potential of intratumoral anti–CTLA-4, anti–PD-1, and anti–4-1BB against bilateral TRAMP-C2.

## Intratumoral combination therapy with CDG elicits skin pathology

In the course of the experiments described above, we observed an inflammatory reaction provoked at the injection site in mice receiving intratumoral administration of CDG together with anti–CTLA-4, anti–PD-1, and anti–4-1BB. Within 2 days of the final therapeutic injection, we observed accumulation of dark, bloody fluid in and around the tumor site that yielded to ulceration, scabbing, and eventual resolution after 2 to 3 weeks. This pathology required concomitant local administration of CDG and checkpoint modulators, as no ulceration occurred following CDG or checkpoint modulation therapy alone. This effect was dose-dependent with respect to the number of CDG doses, with mild inflammation and no ulceration observed in mice that received



**Figure 3.**
Intratumoral combination CDG and checkpoint modulation mobilizes abscopal responses against distal TRAMP-C2. **A,** Five to 8-week-old C57BL/6 mice were challenged with 1 × 10⁶ TRAMP-C2 cells on both flanks, and were treated on days 14, 18, and 22 after implantation with intratumoral CDG and/or checkpoint modulators at the right flank tumor only. **B,** Percentage of mice tumor free at each flank, (**C**) tumor growth kinetics, and (**D**) overall survival over the treatment period are shown. Mice were deemed moribund when tumor volume reached 1,000 mm³. Data are cumulative of n = 3 to 4 experiments with 5 to 10 mice per group. Statistical significance for survival was calculated using the Gehan–Breslow–Wilcoxon test. Ns, not significant; *, P < 0.05; **, P < 0.01; ***, P < 0.001; ****, P < 0.0001.
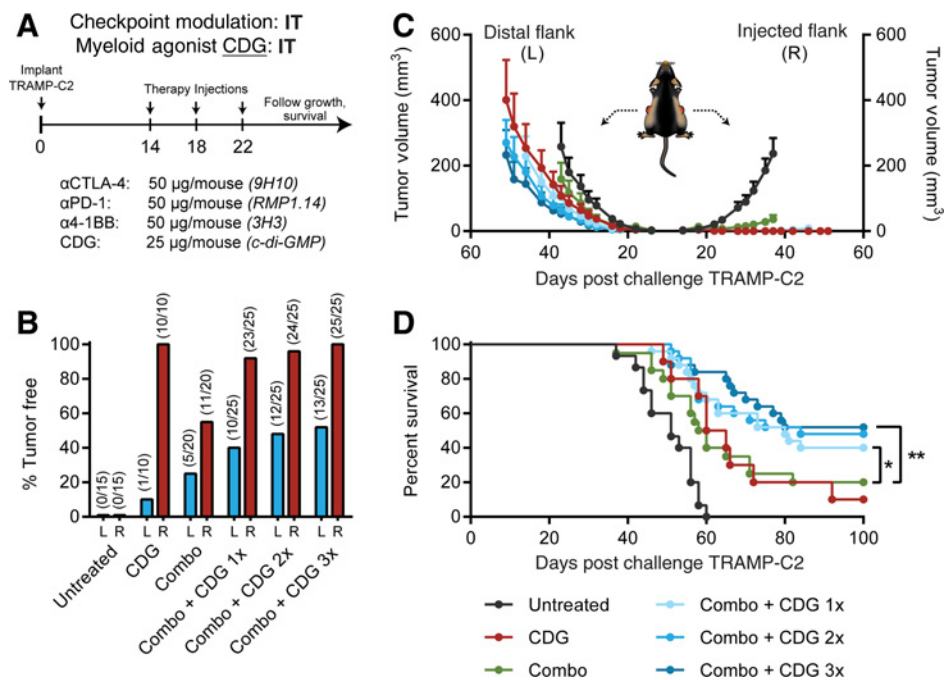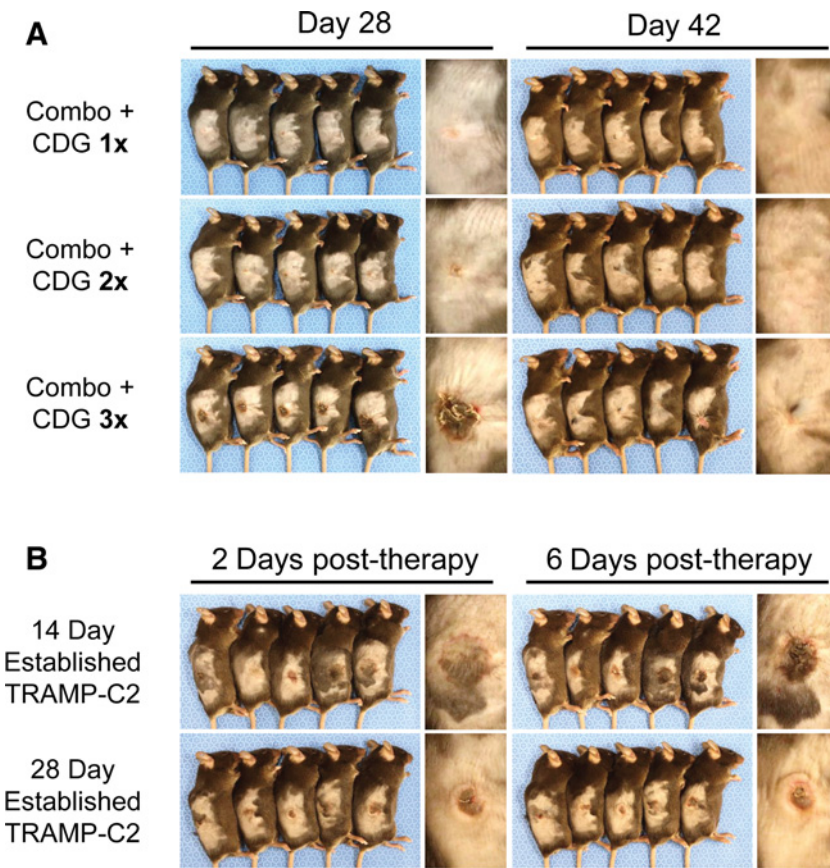
**Figure 4.**
Intratumoral CDG with checkpoint modulation invokes dose-dependent and tumor size-dependent ulcerative pathology at the tumor site. **A,** Photographs of representative mice treated as described in Fig. 3 were taken 6 days following final intratumoral injection (day 28), when ulceration is most intense, and 2 weeks later during the resolution phase (day 42). **B,** Mice bearing either 14-day or 28-day established TRAMP-C2 tumors were given three intratumoral injections of CDG with anti–CTLA-4, anti–PD-1, and anti–4-1BB every 4 days for a total of three injections, according to normal protocol. Photographs of ulceration were taken 2 (day 24) and 6 (day 28) days following final intratumoral injection.

one or two CDG doses (Fig. 4A). Tumor size at the time of therapy may also play a role in determining the extent of ulceration, as injection of larger, 28-day established TRAMP-C2 tumors resulted in reduced ulceration generally localized to the tumor core and not evident in the surrounding skin (Fig. 4B). Given that three concurrent doses of CDG with intratumoral anti–CTLA-4, anti–PD-1, and anti–4-1BB were associated with ulcerative pathology at the injection site yet delivered little survival benefit
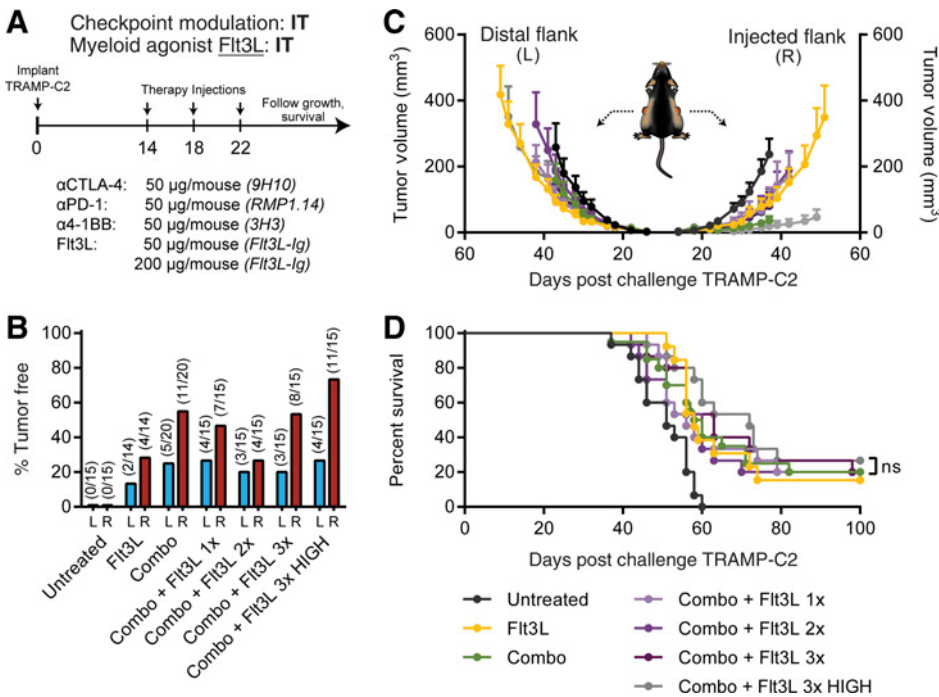


**Figure 5.**
Intratumoral combination Flt3L and checkpoint modulation does not mobilize abscopal responses against distal TRAMP-C2. **A,** Five to 8-week-old C57BL/6 mice were challenged with $1 \times 10^6$ TRAMP-C2 cells on both flanks, and were treated on days 14, 18, and 22 after implantation with intratumoral Flt3L and/or checkpoint modulators in the right flank only. **B,** Percent of mice tumor free at each flank, (**C**) tumor growth kinetics, and (**D**) overall survival over the treatment period are shown. Mice were deemed moribund when tumor volume reached 1,000 mm$^3$. Data are cumulative of $n = 3$ to 4 experiments with 5 mice per group. Statistical significance for survival was calculated using the Gehan–Breslow–Wilcoxon test. ns, not significant; *, $P < 0.05$; **, $P < 0.01$; ***, $P < 0.001$; ****, $P < 0.0001$.

over one or two concurrent CDG doses (Fig. 3D), it may be prudent to limit STING agonist dosing in the combination setting in order to maximize therapeutic benefit while minimizing adverse event frequency and severity.

### Flt3L with checkpoint modulation failed to generate abscopal immunity

Using the treatment schedule described in Figure 5A, we evaluated whether local Flt3L could mobilize abscopal immunity against TRAMP-C2 when combined with intratumoral triple checkpoint modulation. In contrast to CDG, we found that Flt3L failed to synergize with local checkpoint modulation in mediating systemic tumor immunity, delivering no survival benefit over anti–CTLA-4, anti–PD-1, and anti–4-1BB alone (Fig. 5B–D). Given the possibility that the therapeutic potency of our human Flt3L-Ig protein could be limited by sub-optimal receptor binding affinity and generation of neutralizing antibodies, we tested a saturating dose of 200 μg per injection (Fig. 5B–D; Flt3L 3x "HIGH") and found that although local efficacy against the injected tumor was increased, abscopal immunity failed to improve. Of all mice treated, we noted that the incidence of relapse was higher in groups that received intratumoral Flt3L compared with groups treated with CDG, although the results were not statistically significant, and time to relapse was not disparate between these groups (Supplementary Fig. S4). Although these data suggest that in situ vaccination with Flt3L was inferior to CDG in the context of checkpoint modulation, we wished to further confirm that this discrepancy was a generalizable phenomenon and not dependent on tumor size at the time of injection. To address this, we asymmetrically implanted mice with TRAMP-C2 to obtain 28-day established tumors ($\sim$200 mm$^3$) on the right flank and 14-day established tumors ($\sim$20 mm$^3$) on the left flank before beginning local treatment (Supplementary Fig. S5A). Though the long engraftment period led to variability in both tumor size at the right flank and engraftment efficiency of distal tumors by the time of treatment, we were able to observe more effective local control of large TRAMP-C2 tumors following in situ delivery of combination checkpoint modulation and CDG in comparison to local checkpoint antibodies and Flt3L. Despite the inferior regression of the injected lesion, Flt3L did show an equivalent capacity to 3xCDG to promote abscopal responses targeting the smaller, uninjected tumor on the opposite flank (Supplementary Fig. S5B). Together, we conclude that CDG is superior to Flt3L in potentiating local checkpoint modulation to induce both local control and to mobilize abscopal effects against TRAMP-C2 tumors.

### STING/checkpoint therapy increased T-cell infiltration and reduced suppressive myeloid polarization

To further understand the biological mechanisms driving response to intratumoral therapy at both injected and distal TRAMP-C2 tumors, as well as the differential capacity of CDG and Flt3L to potentiate local checkpoint modulation, we utilized 18-color flow cytometry to phenotype and functionally characterize the immune composition of bilateral TRAMP-C2 tumors following intratumoral therapy. As local CDG injection of 14-day established TRAMP-C2 mediates rapid, complete regression leaving minimal tumor tissue for analysis, we allowed tumors to establish for 31 days before initiating therapy, performing intratumoral injections on right flank

tumors on days 31, 35, and 39, and harvesting all tumors on day 42 (Supplementary Fig. S4).

At baseline, TRAMP-C2 tumors are dominated by a dense myeloid infiltrate consisting of CD11b$^+$F4/80$^+$Gr-1$^-$ TAM and CD11b$^+$Gr-1$^+$ MDSCs (Fig. 6B). T cells constitute only 5% of all CD45$^+$ cells and are composed of roughly even proportions of CD8$^+$ cytolytic T lymphocytes (CTL), CD4$^+$FoxP3$^-$ effector T lymphocytes (Teff), and CD4$^+$FoxP3$^+$ Treg (Fig. 6C). Intratumoral CDG administration enhanced CD8$^+$ T-cell infiltration of injected tumors and caused local accumulation of CD11b$^+$Gr-1$^+$F4/80$^{neg}$ granulocytes, likely indicating neutrophil infiltration (Fig. 6D; Supplementary Fig. S7). In contrast, intratumoral Flt3L elicits increased CD11c$^+$CD11b$^-$ DC accumulation, yet triggered expansion of Treg in both injected and uninjected tumors (Fig. 6B and C). Intratumoral checkpoint modulation enhanced the proportion of T cells infiltrating TRAMP-C2 tumors and diminished the Treg pool, likely through antibody-dependent cellular cytotoxic depletion of αCTLA-4–coated Treg (24). Concurrent administration of CDG and checkpoint-modulating antibodies further enhanced CD8$^+$ T-cell accumulation at each tumor, resulting in favorable CD8:Treg ratios that were superior to those seen in response to combination therapy with Flt3L (Fig. 6E). Using tetramer staining to track the known immunodominant SPAS-1 neoepitope expressed in TRAMP-C2 (25), we found that combination therapy with CDG enhanced the density of SPAS-reactive CD8$^+$ T cells at the injected tumor and exhibited a trending capacity to mobilize these cells to the distal tumor, which was not observed in mice receiving Flt3L therapy (Fig. 6F). Local CDG synergized with checkpoint modulation to reduce the percentage of SPAS-specific T cells within the total pool of infiltrating CD8$^+$ T cells, suggesting that this therapeutic approach may diversify the T-cell receptor repertoire to more effectively target subdominant epitopes in addition to SPAS-1 compared with checkpoint modulation alone or combination therapy with Flt3L (Fig. 6G). These data indicate a mechanistic basis underlying the discrepancy in efficacy between local combination therapy incorporating CDG and Flt3L wherein CDG elicits numerous and diverse CD8$^+$ T-cell responses against injected and uninjected tumors, whereas the efficacy of Flt3L is limited by the tendency to promote CD4$^+$ T-cell responses.

The dense myeloid infiltrate characteristic of TRAMP-C2 tumors poses a barrier to the function of infiltrating cytolytic T cells. Even in this context, we found that local priming with 3XCDG promoted improved CD8:TAM ratios relative to the untreated animals (Fig. 6H). This was also evident for 1xCDG vs. Flt3L for CD8:MDSC ratios; however, these data for the 3xCDG group were confounded by the large neutrophil infiltration in response to the skin inflammation shown in Figure 4, and our inability to distinguish these neutrophils from PMN-MDSC using the antibodies in our panel (Supplementary Fig. S7A). Overall though, few, if any, tumors reached ratios at which CD8$^+$ T cells are expected to fully escape myeloid suppression. Therefore, we hypothesize that intratumoral delivery of myeloid agonists can reprogram tumor myeloid populations to reduce their immunosuppressive activity, creating a microenvironment that is amenable to T-cell effector function despite unfavorable relative cellular ratios. Supporting this hypothesis, we observed downregulation of the M2 macrophage marker CD206 on TAM in tumors receiving CDG concurrently with all three doses of anti–CTLA-4, anti–PD-1, and anti–4-1BB, potentially indicating repolarization of TAM in response to CDG combined with checkpoint modulation
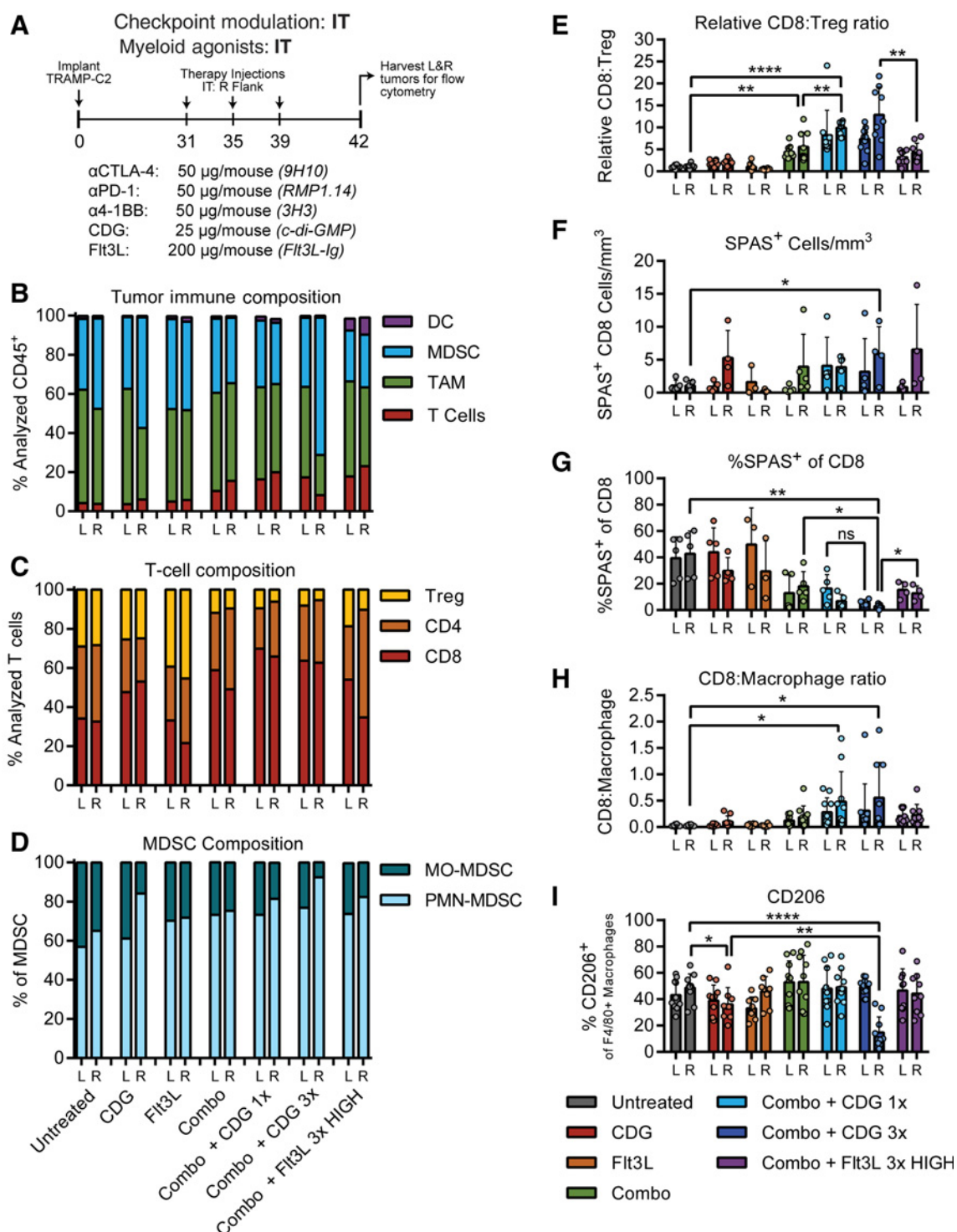
**Figure 6.**

Analysis of the TRAMP-C2 immune infiltrate at local and distal tumors following intratumoral therapy at a single lesion. **A,** To obtain cell numbers sufficient for flow analysis, TRAMP-C2 tumors were established for 31 days, exposed to three doses of intratumoral therapy at the right flank, then were harvested for multiparameter flow cytometry as described in Materials and Methods. See Supplementary Materials for antibodies used and gating strategy. **B,** Relative proportions of unique cell subsets within the CD45$^+$ immune infiltrate, normalized to the total number of gated cells. **C,** Relative proportions of T-cell subsets within the CD3$^+$ lymphocyte infiltrate, normalized to the total number of gated T cells. **D,** Relative proportions of MDSC subsets within the CD11b$^+$Gr-1$^+$ immune infiltrate. **E,** Calculated ratios of CD8$^+$ T cells to Treg, (**F**) density of SPAS-1 tetramer$^+$ CD8$^+$ T cells, (**G**) percentage of SPAS-1 reactive T cells within all infiltrating CD8 T cells, and ratio of CD8$^+$ T cells to (**H**) macrophages are shown. **I,** Percentage of macrophages expressing the M2 macrophage marker CD206. Data are cumulative of 2 independent experiments with 5 mice per group. Statistical significance was calculated using the Student $t$ test. ns, not significant; *, $P < 0.05$; **, $P < 0.01$; ***, $P < 0.001$; ****, $P < 0.0001$.

(Fig. 6I). Although combination therapy with Flt3L promoted DC expansion and a reduction in MDSC populations, Flt3L failed to induce CD206 downregulation on TAM, suggesting this effect is specific to CDG. We conclude, therefore, that relative to Flt3L, CDG better potentiates intratumoral anti–CTLA-4, anti–PD-1, and anti–4-1BB activity by increasing infiltration and diversification of tumor-specific CD8$^+$ T cells at local and distal tumors, enhancing CD8:Treg ratios, and by reprogramming suppressive TAM to a proinflammatory phenotype.

## Discussion

Simultaneous manipulation of multiple, nonredundant immune regulatory systems can activate potent antitumor immune responses in mouse and man. Translation of this approach, however, has been limited by cumulative inflammatory side effects, which limit the tolerability of high-order combination therapies in patients. At the time of this writing, the only combination immunotherapy with FDA approval consists of ipilimumab (Yervoy; anti–CTLA-4) and nivolumab (Opdivo; anti–PD-1) for patients with *Braf* V600 wild-type unresectable or metastatic melanoma. Though effective and tolerable in this indication, a number of solid tumors, including CRPC, remain resistant to these therapies. We report that an optimized cocktail of immunomodulators engaging both innate and adaptive immunity mediates efficient rejection of poorly immunogenic murine prostate cancer. Although local stimulation of the STING or Flt3 pathways can complement checkpoint-modulating antibodies targeting CTLA-4, PD-1, and 4-1BB to delay tumor growth and enhance survival of mice with multifocal TRAMP-C2, we find that the STING agonist CDG mobilizes abscopal immunity more efficiently than Flt3L. In an effort to mitigate the toxicity of these high-order combinations, we report that intratumoral injection of low-dose checkpoint modulators together with CDG, but not Flt3L, is sufficient to induce curative abscopal immunity in approximately 50% of mice. We identify a potential mechanistic basis for the discrepancy in synergy between checkpoint modulators and CDG vs. Flt3L, as CDG promotes CD8 skewing, infiltration of tumor-specific T cells, and enhanced intratumoral ratios of CD8$^+$ T cells to Treg, TAM, and MDSC, whereas Flt3L facilitates expansion of CD4 T cells, including Treg, in both local and distal tumors. Combination therapy with CDG may reduce the suppressive capacity of TAM in TRAMP-C2 tumors, as we observe downregulation of the M2 macrophage marker CD206 in response to this therapy. These data suggest that STING-mediated myeloid programming can potentiate intratumoral T-cell checkpoint modulation to render multifocal prostate cancer sensitive to immunotherapy.

Abscopal effects are the holy grail of intratumoral therapy. Although published reports describe regression of uninjected lesions in response to local delivery of STING-activating cyclic dinucleotides (CDN), we find that single-agent CDG fails to elicit abscopal immunity against distal TRAMP-C2 tumors (15). This discrepancy may be related to the type of CDN used, as CDG binds with low affinity to STING yet can engage the inflammasome to promote IL1β production, unlike synthetic CDNs used in other studies (26). Furthermore, this may be a product of the TRAMP-C2 model resulting from genomic DNA being leaked into the cytoplasm to trigger low levels of chronic STING signaling by this cell line (27). This, in turn, may promote interferon-induced expression of PD-L1 and indolea-

mine 2,3-dioxygenase in the microenvironment that can act as barriers to immune responses generated at distant sites. Our results suggest that the capacity for STING agonists alone to elicit abscopal effects is limited in certain indications. Nevertheless, even in this context, we demonstrate that abscopal immunity can be effectively mobilized when CDNs are administered in combination with checkpoint modulation.

Although intratumoral therapy carries the benefit of minimizing off-target toxicities common in patients receiving systemic immunotherapy, overt inflammation at the injection site can complicate dosing strategies of locally administered agents. We observe an ulcerative response to intratumoral therapy in mice receiving combination CDG and anti–CTLA-4, anti–PD-1, and anti–4-1BB; delivery of CDG or checkpoint modulators alone does not elicit this pathology. Baird and colleagues have also reported intratumoral hemorrhagic necrosis in a number of tumor models upon local delivery of R$_p$, R$_p$ dithio-CDG (RR-CDG) with radiotherapy, involving swelling and leakage of neovascular endothelium and stromally derived TNFα release (28). We observe accumulation of CD11b$^+$Gr-1$^+$F4/80$^-$ granulocytes in these tumors, suggesting inflammatory neutrophils may be contributing to ulceration, possibly through production of TNFα. Ulcerative pathology appears less extensive in larger tumors, although it is unknown whether this is due to the presence of larger numbers of suppressive TAM and MDSC, vascular constriction due to stromal desmoplasia in advanced TRAMP tumors, or reduced bystander activation of cells in surrounding healthy skin. By reducing the number of CDG doses administered concurrently with checkpoint modulators, we observe reduction in local ulceration without sacrificing therapeutic power as measured by distal tumor growth or overall survival. Therefore, we conclude that combination therapies incorporating STING agonists with intratumoral checkpoint modulators can promote localized tissue pathology, and that an optimal therapeutic index may be reached by restricting CDN dosing.

High-order combinations of immunotherapies that engage both innate and adaptive immunity have the potential to regress preclinical models of aggressive, poorly immunogenic cancer, but cumulative inflammatory toxicities can impede translation of these therapies into patients. We evaluated a cocktail of T-cell checkpoint–modulating antibodies targeting CTLA-4, PD-1, and 4-1BB together with intratumoral innate agonists engaging either STING or Flt3 in a poorly immunogenic model of multifocal murine prostate cancer. In the context of systemic checkpoint modulation, intratumoral CDG or Flt3L deliver curative responses in the majority of mice; however, CDG proves to be the best choice to augment intratumoral low-dose combination checkpoint blockade. Although this intratumoral combination therapy can induce injection site ulcerative pathology, limiting CDG dosing can sustain tissue integrity without foregoing survival benefit, illuminating an avenue by which high-order combination immunotherapy can be delivered for systemic control of poorly immunogenic prostate cancer with reduced local and systemic toxicity.

### Disclosure of Potential Conflicts of Interest

No potential conflicts of interest were disclosed.

### Disclaimer

The content is solely the responsibility of the authors and does not necessarily represent the official views of the NIH.

## Authors' Contributions

**Conception and design:** C.R. Ager, M.A. Curran

**Development of methodology:** C.R. Ager, M.A. Curran

**Acquisition of data (provided animals, acquired and managed patients, provided facilities, etc.):** C.R. Ager, M.J. Reilley, C. Nicholas, T. Bartkowiak, A.R. Jaiswal

**Analysis and interpretation of data (e.g., statistical analysis, biostatistics, computational analysis):** C.R. Ager, M.J. Reilley, T. Bartkowiak, A.R. Jaiswal, M.A. Curran

**Writing, review, and/or revision of the manuscript:** C.R. Ager, M.J. Reilley, T. Bartkowiak, M.A. Curran

**Administrative, technical, or material support (i.e., reporting or organizing data, constructing databases):** C.R. Ager, C. Nicholas

**Study supervision:** M.A. Curran

## Acknowledgments

## Grant Support

## References

1. Kwon ED, Drake CG, Scher HI, Fizazi K, Bossi A, van den Eertwegh AJM, et al. Ipilimumab versus placebo after radiotherapy in patients with metastatic castration-resistant prostate cancer that had progressed after docetaxel chemotherapy (CA184-043): a multicentre, randomised, double-blind, phase 3 trial. Lancet Oncol 2014;15: 700–12.
2. Topalian SL, Hodi FS, Brahmer JR, Gettinger SN, Smith DC, McDermott DF, et al. Safety, activity, and immune correlates of anti–PD-1 antibody in cancer. N Eng J Med 2012;366:2443–54.
3. Ritch CR, Cookson MS. Advances in the management of castration resistant prostate cancer. BMJ 2016;355:i4405.
4. Foster BA, Gingrich JR, Kwon ED, Madias C, Greenberg NM. Characterization of prostatic epithelial cell lines derived from transgenic adenocarcinoma of the mouse prostate (TRAMP) model. Cancer Res 1997;57:3325–30.
5. Gabrilovich DI, Ostrand-Rosenberg S, Bronte V. Coordinated regulation of myeloid cells by tumours. Nat Rev Immunol 2012;12:253–68.
6. Curran MA, Montalvo W, Yagita H, Allison JP. PD-1 and CTLA-4 combination blockade expands infiltrating T cells and reduces regulatory T and myeloid cells within B16 melanoma tumors. Proc Nat Acad Sci U S A 2010;107:4275–80.
7. Wolchok JD, Kluger H, Callahan MK, Postow MA, Rizvi NA, Lesokhin AM, et al. Nivolumab plus ipilimumab in advanced melanoma. N Engl J Med 2013;369:122–33.
8. Larkin J, Chiarion-Sileni V, Gonzalez R, Grob JJ, Cowey CL, Lao CD, et al. Combined nivolumab and ipilimumab or monotherapy in untreated melanoma. N Engl J Med 2015.
9. Curran MA, Kim M, Montalvo W, Al-Shamkhani A, Allison JP. Combination CTLA-4 blockade and 4-1BB activation enhances tumor rejection by increasing T-cell infiltration, proliferation, and cytokine production. PLoS One 2011;6:e19499.
10. Maraskovsky E, Brasel K, Teepe M, Roux ER, Lyman SD, Shortman K, et al. Dramatic increase in the numbers of functionally mature dendritic cells in Flt3 ligand-treated mice: multiple dendritic cell subpopulations identified. J Exp Med 1996;184:1953–62.
11. Salmon H, Idoyaga J, Rahman A, Leboeuf M, Remark R, Jordan S, et al. Expansion and Activation of CD103(+) dendritic cell progenitors at the tumor site enhances tumor responses to therapeutic PD-L1 and BRAF inhibition. Immunity 2016;44:924–38.
12. Klein O, Ebert LM, Zanker D, Woods K, Tan BS, Fucikova J, et al. Flt3 ligand expands CD4+ FoxP3+ regulatory T cells in human subjects. Eur J Immunol 2013;43:533–9.
13. Woo SR, Fuertes MB, Corrales L, Spranger S, Furdyna MJ, Leung MY, et al. STING-dependent cytosolic DNA sensing mediates innate immune recognition of immunogenic tumors. Immunity 2014;41:830–42.
14. Fu J, Kanne DB, Leong M, Glickman LH, McWhirter SM, Lemmens E, et al. STING agonist formulated cancer vaccines can cure established tumors resistant to PD-1 blockade. Sci Transl Med 2015;7:283ra52.
15. Corrales L, Glickman LH, McWhirter SM, Kanne DB, Sivick KE, Katibah GE, et al. Direct activation of STING in the tumor microenvironment leads to potent and systemic tumor regression and immunity. Cell Rep 2015;11: 1018–30.
16. Bartkowiak T, Curran MA. 4-1BB agonists: multi-potent potentiators of tumor immunity. Front Oncol 2015;5:117.
17. Curran MA, Allison JP. Tumor vaccines expressing Flt3 ligand synergize with CTLA-4 blockade to reject preimplanted tumors. Cancer Res 2009; 69:7747–55.
18. Boutros C, Tarhini A, Routier E, Lambotte O, Ladurie FL, Carbonnel F, et al. Safety profiles of anti-CTLA-4 and anti-PD-1 antibodies alone and in combination. Nat Rev Clin Oncol 2016;13:473–86.
19. Segal NH, Logan TF, Hodi FS, McDermott DF, Melero I, Hamid O, et al. Results from an integrated safety analysis of urelumab, an agonist anti-CD137 monoclonal antibody. Clin Cancer Res 2016;23: 1929–36.
20. Hodi FS, O'Day SJ, McDermott DF, Weber RW, Sosman JA, Haanen JB, et al. Improved survival with ipilimumab in patients with metastatic melanoma. N Eng J Med 2010;363:711–23.
21. Topalian SL, Hodi FS, Brahmer JR, Gettinger SN, Smith DC, McDermott DF, et al. Safety, activity, and immune correlates of anti-PD-1 antibody in cancer. N Eng J Med 2012;366:2443–54.
22. Fransen MF, van der Sluis TC, Ossendorp F, Arens R, Melief CJ. Controlled local delivery of CTLA-4 blocking antibody induces CD8+ T-cell-dependent tumor eradication and decreases risk of toxic side effects. Clin Cancer Res 2013;19:5381–9.
23. Marabelle A, Kohrt H, Sagiv-Barfi I, Ajami B, Axtell RC, Zhou G, et al. Depleting tumor-specific Tregs at a single site eradicates disseminated tumors. J Clin Invest 2013;123:2447–63.
24. Simpson TR, Li F, Montalvo-Ortiz W, Sepulveda MA, Bergerhoff K, Arce F, et al. Fc-dependent depletion of tumor-infiltrating regulatory T cells co-defines the efficacy of anti-CTLA-4 therapy against melanoma. J Exp Med 2013;210:1695–710.
25. Fasso M, Waitz R, Hou Y, Rim T, Greenberg NM, Shastri N, et al. SPAS-1 (stimulator of prostatic adenocarcinoma-specific T cells)/SH3GLB2: A prostate tumor antigen identified by CTLA-4 blockade. Proc Natl Acad Sci USA 2008;105:3509–14.
26. Abdul-Sater AA, Tattoli I, Jin L, Grajkowski A, Levi A, Koller BH, et al. Cyclic-di-GMP and cyclic-di-AMP activate the NLRP3 inflammasome. EMBO Rep 2013;14:900–6.
27. Ho SS, Zhang WY, Tan NY, Khatoo M, Suter MA, Tripathi S, et al. The DNA structure-specific endonuclease MUS81 mediates DNA sensor STING-dependent host rejection of prostate cancer cells. Immunity 2016;44: 1177–89.
28. Baird JR, Friedman D, Cottam B, Dubensky TW Jr., Kanne DB, Bambina S, et al. Radiotherapy combined with novel STING-targeting oligonucleotides results in regression of established tumors. Cancer Res 2016; 76:50–61.